

How a combination of innovative methods can help for the development of new deodorant Products

Sylvie Marull-Tufeu*, Julie Ongenaed ; Caroline Goelettes-Seclet ; Eric Fernandez ; Emilie Jacques

Direction Innovation & Développement, Laboratoire Application Cutanée & Consommateurs, Yves Rocher, Issy les Moulineaux, France

*Sylvie Marull-Tufeu, 7 chemin de Bretagne, 92130 Issy-Les-Moulineaux, France

Tel : +33-(1)41085952

Email: sylvie.marull-tufeu@yrnet.com

Abstract

Background: Sweating is an essential process to maintain the human body at an optimal temperature. Nevertheless, it may induce two major inconveniences during the day: wet sensation and malodor. This is why we developed a deodorant development strategy oriented through humidity sorption and malodor coverage with fragrances.

Methods: Humidity sorption and desorption studies were conducted on several powders by quantifying the maximal amount of liquid absorbed by powder before saturation and gravimetry respectively.

We characterized with Environmental Scanning Electron Microscopy (ESEM) the shape and behavior of selected powders under humidity.

Sweat sampling from volunteers was analyzed using an electronic nose technology. Comparison of untreated and treated sweat allowed us to compare the efficacy of fragrance in masking odor.

Self-assessment of the deodorant with different fragrances were proposed to the volunteers for appreciation.

Results: We were able to select a powder presenting a good absorption of (artificial) sweat, and a low rate of desorption. Under ESEM observation, selected powder (C) showed a fibers morphology and ability to swell with humidity.

We observed, with electronic nose, a variability of sweat signal between volunteers, and a kinetic evolution of sweat. We were then able to assess the efficiency of fragrances in masking odor by activating new sensors, generating a new odor.

Conclusion: A progressive strategy of test using methods has been developed to select ingredients in the early steps of deodorant development.

Key words: deodorant; sweat; Environmental Scanning Electron Microscopy: Electronic Nose

Introduction

Sweating is an essential process to maintain the human body at an optimal temperature. Nevertheless, even with a good body hygiene, sweating may induce two major inconveniences during the day: wet sensation and malodor. Excessive sweat can be induced by different parameters such as high environmental temperature or stress.

Sweat, is the result of the secretion of two kinds of glands: eccrine and apocrine.^[1]

Apocrine glands are specifically localized in armpit, lid, mammary and genital area, stimulation is mostly activated by emotions. The liquid secreted is viscous and contains electrolytes, steroids, proteins, lipids. This secretion, presenting initially no odor, will be metabolized by armpit bacteria, and the volatile molecule obtained, will generate sweat odor, currently associated to malodor.^[2]

The armpit area is propitious to bacterial proliferation due to gland production, the humidity is high and nutriments for bacterial survival and development are abundant.

Furthermore, the kind of odor is very dependent on the individuals, and varies according to stimuli, physical activity, genetic, food habits. The microflora population varies from one individual to the other, even if the majority of person have armpits colonized with staphylococci, aerobic coryneform, and to a lesser extent with propionibacteria,^[3] which is also an important parameter in malodor generation.

Knowing the mechanism of sudation, we can act on different parameters such as reducing humidity, limiting bacterial proliferation, masking odor.

Firstly, we investigated the capability of ingredients such as natural powders to reduce the level of sweat available in the armpit area by retaining it through mechanisms such as absorption and/or adsorption.

Humidity sorption and desorption studies were conducted on several powders by quantifying the maximal amount of artificial sweat solution absorbed before saturation and by following releasing of water via gravimetric measurements. These results lead us to a selection.

To go further, selected powders were studied using Environmental Scanning Electron Microscopy (ESEM). Electron microscopy permitted the characterization of individualized particles, while the Environmental mode allowed to control the relative humidity inside the microscope chamber. Thus, the evolution of particles during hydration and dehydration processes were followed in real time.

To go further in the understanding of water absorption and retention, we chose to observe 2 powders with contrasting behavior towards artificial sweat and tried to understand the phenomenon at a microstructure level.

We observed the initial microstructure of the powders then we observed the apparent changes in microstructure during hydration using ESEM. We were able to observe in real time the effect of increasing humidity in the chamber on the aspect of the powder particles.

Secondly, we explored an original screening approach to compare different fragrances in their ability to mask malodor from sweat.

In this purpose we worked with a new technology based on surface plasmon resonance able to transform one or a mix of volatile molecules into an olfactive profile.

First of all, we studied with this method the variability of sweat signals from different volunteers immediately after collecting, and after an incubation time.

Finally, we compared the ability of different fragrances into a deodorant formula, to modify this sweat profile. We started from the assumption that the most effective fragrance should be able to transform enough the sweat odor to have a different profile than the untreated sweat.

Since we can't associate the profile measured with a hedonic perception, we also compared the perception of efficacy via a consumer self-evaluation of body malodor using this fragrance into a deodorant formula.

Materials and methods

Sweat absorption analysis:

We assessed the ability of 6 Natural powders, referenced A to G, to absorb water.

The protocol is inspired by the ISO method (*ISO 787-5:1980: General methods of test for pigments and extenders — Part 5: Determination of oil absorption value*), whereas oil is replaced by a synthetic sweat solution.

The principle of the method is based on addition of synthetic sweat solution from a burette to the test portion. We chose a model of artificial sweat solution composed of purified water and salts as described in ISO method referenced as *ISO 105-E04:2008 Textiles -test of color fastness- Part E04: color fastness to perspiration*. The pH of the solution is adjusted to 5.5.

After each addition, the solution is rubbed into the product until conglomerates are formed. The addition of solution is stopped when a paste of smooth consistency has been formed. It should just spread without cracking or crumbling. The volume is read on the burette and the quantity of solution used noted. The result is expressed in grams of sweat per gram of powder.

The aspect of the powder cluster before and after sweat absorption is described.

Sweat desorption analysis:

To quantify the desorption rate, the paste obtained after the saturation of powder by sweat was placed on a balance, in a petri dish, in a chamber at 37°C. The weight of the sample was followed for 7 hours. The rate of desorption was expressed as the % of loss of weight comparing to initial weight.

Dynamic humidity absorption observation by ESEM:

The ESEM equipped with a gaseous secondary electron detector was used to observe the changes in microstructure of samples during hydration. Dry sample was mounted onto aluminum stubs using double-sided adhesive tape. Samples were inserted into the microscopy chamber. The temperature of the ESEM chamber is regulated by a Peltier stage and set up at 2°C. The pressure value is expressed in Torr by the equipment. The initial chamber pressure was below the pressure of water vapor (4 Torr). The working distance between the samples and the detector was 8.2 mm. A 20-kV beam accelerating voltage was applied. The magnification

of ESEM images was 500x. The hydration inside the chamber was gradually increased to induce water condensation on the surfaces. The pressure increased by 0.05 torr every 2 minutes under conditions of vapor condensation in the ESEM chamber. The surface image was taken before each pressure rise. During pressure stabilization, voltage was cut off to prevent the sample from heating up. After reaching the condensation of water, the reverse operation was carried out until the pressure of 4 Torr.

Volatile organic compounds (VOC) analysis by electronic nose: impact of fragrance on the sweat malodor by covering effect:

The electronic nose technology used for this study combines biochemical sensors and a model of data analysis.

An association of 64 biochemical nanosensors composed of peptides are able to link to VOC, depending on their affinity.

Nanosensors are grafted on a micro-optical network (photonic on silicium). Interferences between a light source and the complex captor-fixed volatile molecules are measured by a photo detector.

Each odor, each fragrance, is the sum of different volatiles molecules and has its specific profile. That is why we can compare all the profiles by graph representation related to the 64 sensors.

With this technology, we compared the masking odor effect of 3 fragrances A, B, C, integrated in a deodorant base.

For that purpose, 5 volunteers (men and women from 25 to 55) gave their consent to participate to this study.

Volunteers were asked to provide a physical effort (outdoor running) in order to produce an excess of sudation.

They were requested not to use antiperspirant or eat spicy 24 hours before the study.

Sweat sampling was performed immediately after physical effort. Sweat was collected by application of a sterile swab on armpit areas of the volunteers. 4 samples were collected on the same armpit for each panelist and weighted.

For each panelist one sample remained untreated to follow the signal of natural sweat. A quantity of 0.25g of deodorant with fragrance A, B, or C for 0.02 ml of sweat was applied on the 3 other swabs respectively. Swab were introduced in a glass vial and placed into a chamber at 37°C in order to generate the malodor by bacterial process.

At the beginning to understand the variability between individuals we analyzed the sweat signals samples after 6h at 37°C; before checking previously that the sample present malodor.

Then, we measured sweat signal from T0, T6h to T24h at 37°C to follow the evolution in time.

Finally, we compared signals of untreated vs treated samples by deodorant containing A, B, C fragrance to determine which combination sweat-fragrance generates the most different profile from natural sweat profile presenting a bad odor. (For more convenient reason, we will call the 3 deodorants: Fragrance A, Fragrance B and Fragrance C). Different measurements by sample were taken to ensure repeatability.

Self-appreciation of fragrance on volunteers

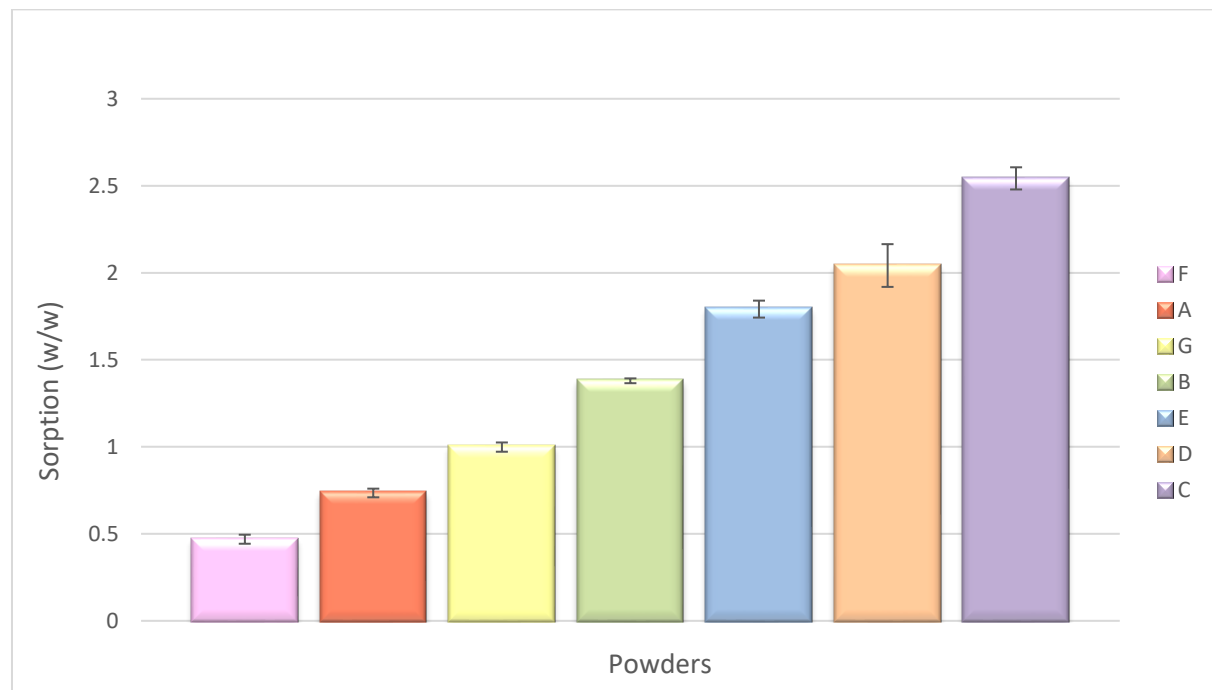
10 volunteers (women aged 22 to 50) gave their informed consent to take part in the test. In the inclusion criteria they had to be regular users of deodorant and not users of antiperspirant.

They were asked not to use deodorant the day of the test and to have their last shower the day before the test.

5 samples, including 3 deodorants formulated with fragrances A, B and C were given to each volunteer. They used deodorant A to E (with randomization), one different per morning. They were invited to answer a questionnaire at the end of the test, giving appreciation regarding efficacy of the samples (intensity after application, evocation of freshness and fragrance appraisal).

Results and discussion:

Sweat/ humidity absorption:



Graph 1: classification of the level of sweat absorption, in g of powder /g of sweat

A classification of the level of absorption in g of sweat/g of powder is made.

Different behaviors are observed.

With powder C the artificial sweat solution is added progressively until a state of saturation. A paste is formed, if pressed, a bit of humidity appears.



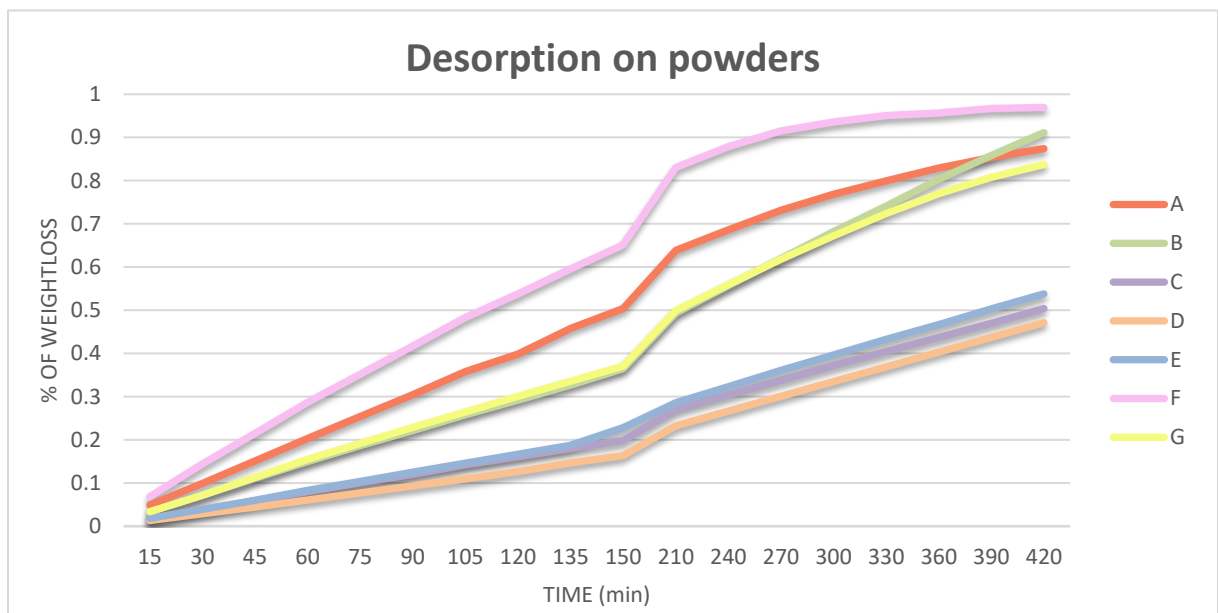
Photography of powder C, before sweat addition (a), during the mix with sweat (b), at sweat saturation (c)

We observed a different phenomenon for F powder which is rapidly saturated with the sweat and doesn't seem to swell.

For powder B, the ability to absorb the liquid was medium, but once the saturation reached, paste had a wet aspect, liquid appeared on the surface, as the desorption started.

Sweat/ humidity desorption:

We noted the initial weight corresponding to the previous paste formed with powders and maximal quantity of sweat absorbed. We followed the weight and express the result as a % of lost weight comparing to initial weight. Gravimetric measurements were taken every 15 minutes for 150 minutes, and then every 30 minutes until 7h.



Graph 2: Rate of desorption, % of weight loss

Compared to others the powder F shows the highest rate of desorption. Powder C presents the lower desorption speed, at the end of the 7hours, they lost less than 50% of their weigh.

Despite the high level of absorption, powder B let the water leaves more quickly than powder C.

For that reason, we selected powder C, as a promising candidate to include in a deodorant, in fact, it has a high level of sweat absorption and a slow sweat release compared to the other powders.

Dynamic humidity absorption observation by ESEM:

We decided to go further by analyzing 2 selected powder at a microscopic level under growing humidity. We chose the best candidate, C presenting a high absorption level and low desorption. F was also selected due to its very low level of humidity absorption and high desorption rate.

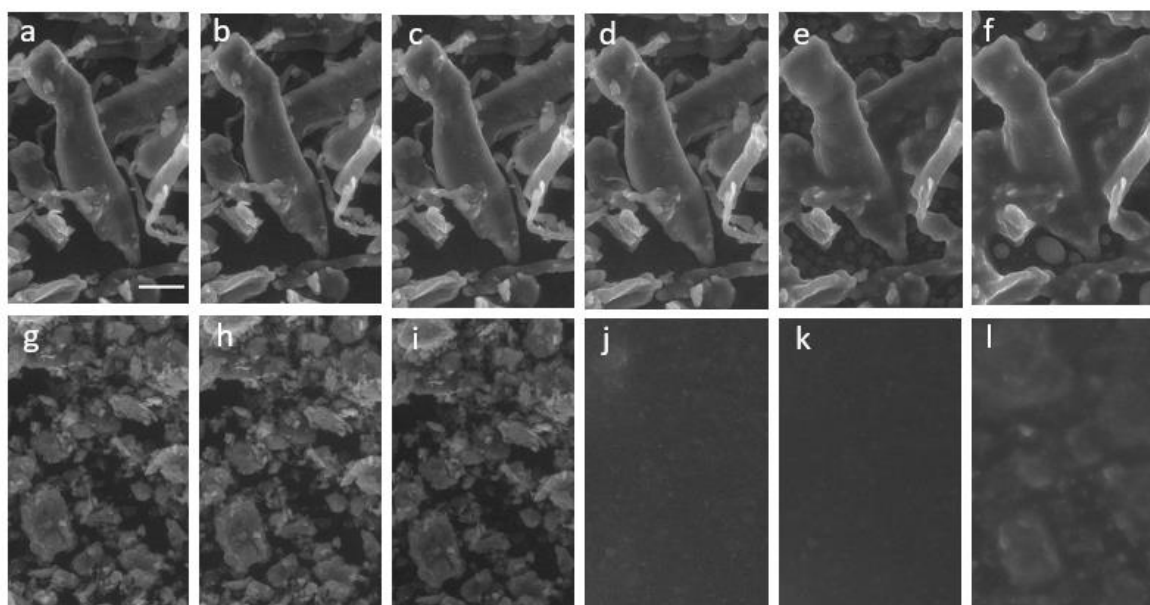


Fig 1- Characterization of microstructure changes of powder C and powder F particles during pressure rise by environmental scanning electron microscopy, at 500x magnification. a to f powder C. g to l powder F. a & g 5,4 Torr -b & h 5.45 Torr- c & I 5,5 Torr – d & j 5,55 Torr – e & k 5,6 Torr – f & l 5,65 Torr. Scale bar 20 μ m

Powder C appears composed of fibers. These fibers show a large variability in size and shape, but the boundaries are relatively well defined. The fibers do not seem to exceed 100 μ m in length but the width can fluctuate within a single fiber and between fibers as well. At the same magnification particles of powder F are smaller and have a spherical shape (not shown at high magnification).

Figure 1 (a) to (f) illustrates the sequence of hydration for powder C. During the rise in pressure, a modification of the morphology of the fibers can be observed. The fibers get bigger. This swelling kinetics is observed gradually from 5.40 to 5.65 Torr. Note that the water saturation in

the ESEM chamber is reached at 5.35 Torr. At a pressure of 5.60 Torr, water droplets appear on the surface of the fibers, and carbon tape. The fibers appear swollen 28 min after the start of hydration. At the next pressure level, the water is still present in greater quantity, but the water remains localized in the vicinity of the fibers. This increase in fiber volume is attributed to water absorption. During drying, the water disappears and the volume of the fibers decreases. The shape of the fibers is very similar to their original state.

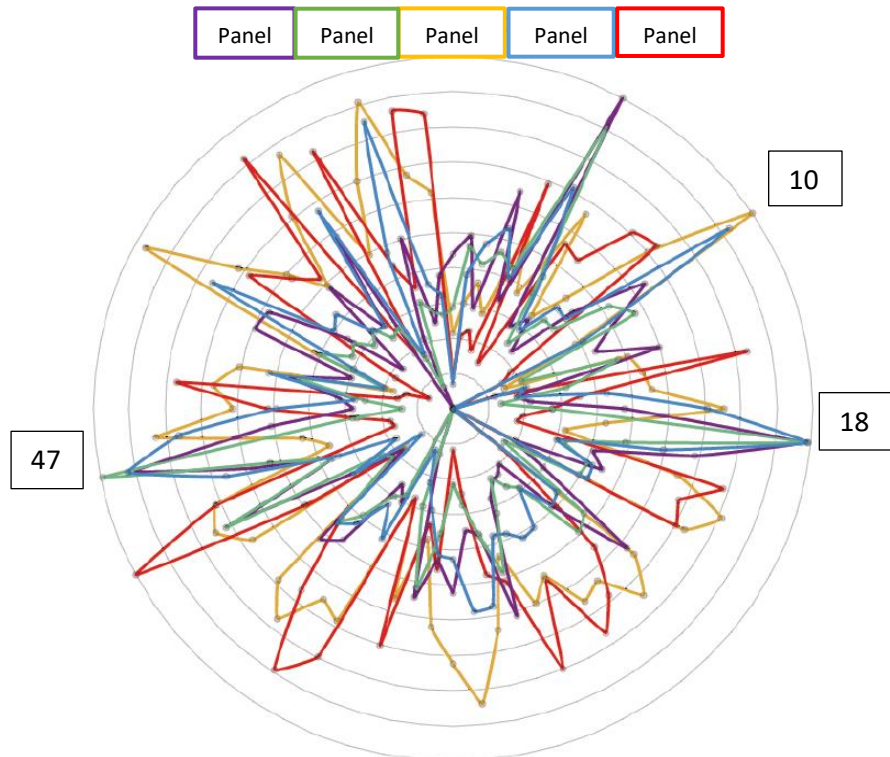
Figure 1 (g) to (l) illustrates the sequence of hydration of powder F. At the difference of powder C, for F, the water arrives earlier on the stub, at 5.55 Torr. The water spreads very quickly until it covered almost the entire field of observation. During the decrease step of pressure, the water disappears but the aspect is different from the initial state. Not at the particle level, but the particle aggregates seem more compact.

VOC analysis by electronic nose: impact of fragrance on the sweat malodor by covering effect:

Results are expressed on a normalized radar chart representing all the 64 sensors. Intensity measured for a sensor reflects the level of VOC that has been linked to this sensor.

At T6h, we observe, for each volunteer, a specific profile, showing a variability inter individuals in terms of sweat composition (excited sensors) and quantity (signal intensity).

Regarding the variability inter individuals, we can confirm there is a personal radar with molecules in affinity to certain sensor more than others (graph 3).

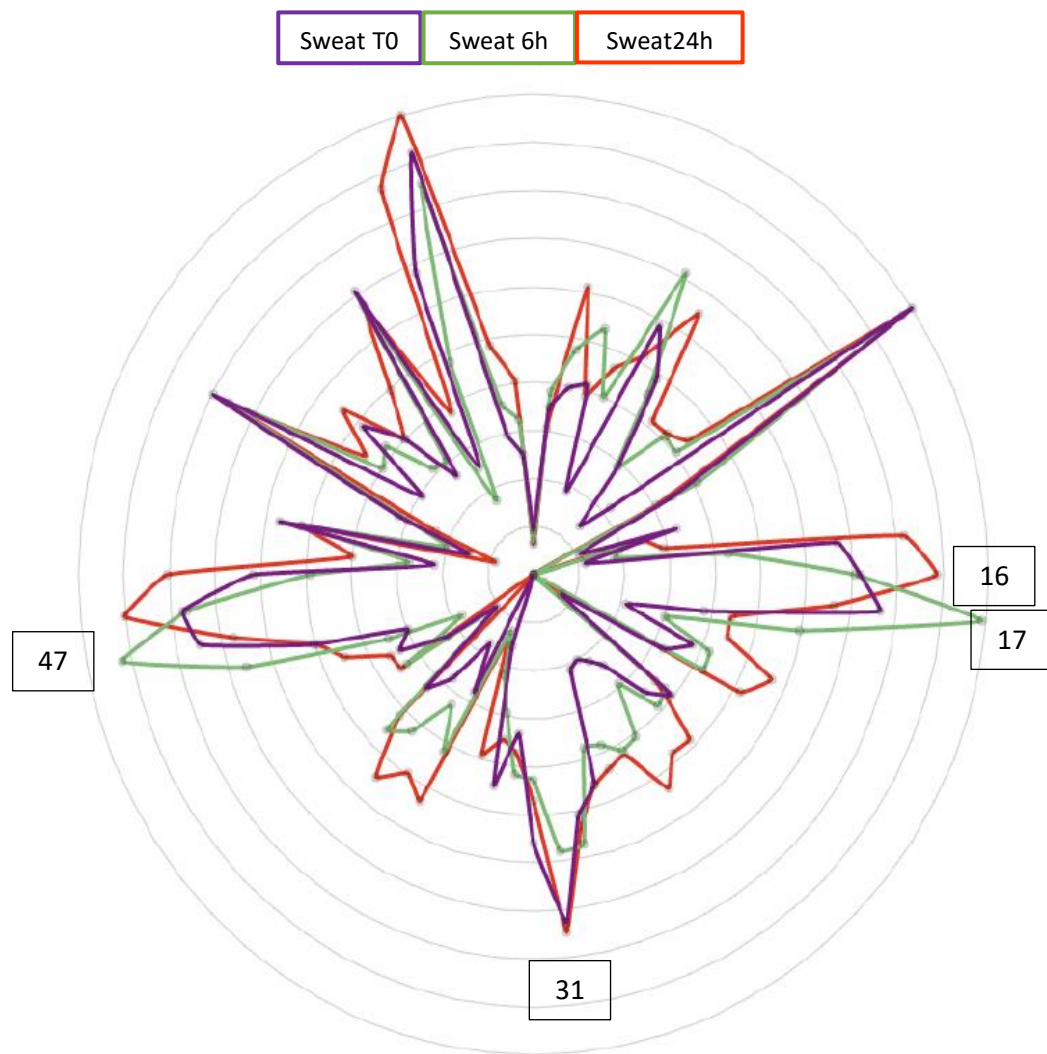


Graph 3: variability of olfactory signal between sample of panel 1,2,3,4,5, 6h at 37°C

Nevertheless, some peaks (10/18/47) are present in all profiles.

To follow the evolution of sweat profile over time, we focused on the profile of untreated sweat of panel 4 by comparing data at T0, T6h and 24h (graph 4). For this volunteer, we can observe that volatiles are linked particularly to sensors 10, 15, 17, 31, 46, 47, 53, 61 at T0. This characteristic signal was present initially, but the kinetic measurements showed a growing intensity appearing at T6h and more intensely at T24H on sensor 16, 17, 31, 47.

We can relate this evolution into to the progressive apparition of odorant volatile molecule, produced by bacterial metabolism.

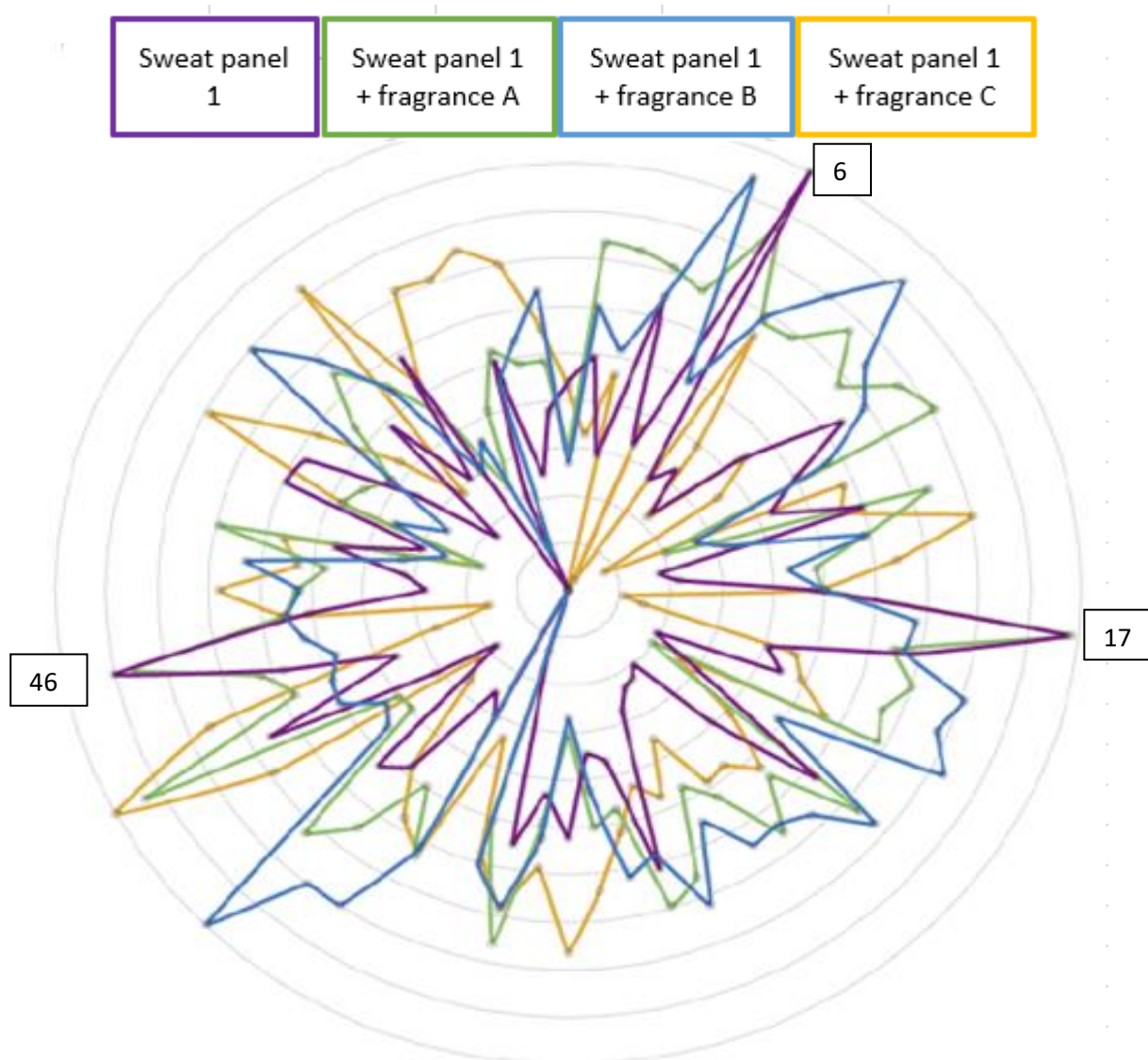


Graph 4: Olfactive profile of panel's sweat n°4. Kinetic evolution of sweat signal

We analyzed the behaviors of the sweat samples in contact with the different deodorants (Fragrance A, B and C) after 6h at 37°C.

We superimposed profile of sweat and profiles of same sweat sample with the different fragrances. We assumed that if the profiles are different with the addition of the fragrances, the latter has the ability to cover sweat odor.

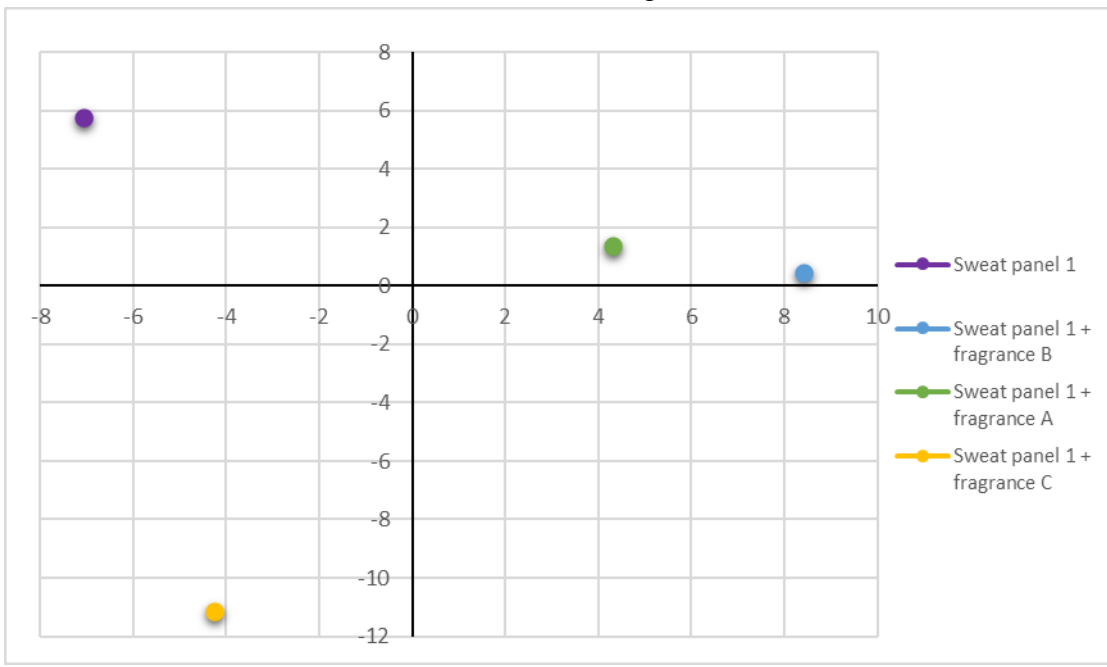
A representation of sweat profile of panelist 1 after 6h showed the transformation of olfactory signature with addition of fragrances A, B or C (graph 5). For every combination “sweat- fragrance”, some peaks already present in sweat signal grew in intensity and other peaks appeared, when new sensors were solicited. Each combination has its own signature.



Graph 5: Olfactive signal of sweat after 6h at 37°C, with and without deodorant to mask odor, panel 1

Focusing on panel 1, untreated sweat radar shows the most important signals measured on sensor 6,17 and 46. When deodorant B for example, is mixed with sweat, we can observe that the resulting profile induces new molecules occurrence in affinity to different sensors than sweat alone 4,8,19,21,40,55.

The principle of masking odor might be induced by the ability to generate a new odor with an intensity high enough to cover the malodor. It corresponds to the new profile of treated sweat. To evaluate the fragrance with the most efficacy in its capacity of masking odor, we represented on PCA (Principal Component Analysis), the data of untreated sweat and sweat combined with fragrances. The more different olfactive signal are, the more plots on PCA will be distant. Graph 6 is the representation using PCA of the data for panel 1. It allows us to calculate distances between olfactive profiles, including all the data for each sensor and conditions. We are then able to evaluate the distance between 2 signals.



Graph 6: PCA for panel 1, spatial representation of untreated and treated sweat with fragrance A, B, C

This methodology allows us to compare for each panelist, which product/fragrance, transforms the most the signal of sweat. As each volunteer has its own profile, we analyzed the data separately and observed for the different panelists which fragrance appears more different (meaning distant on the PCA) than their untreated sweat profile. We obtain a majority of volunteers with the higher distance between their untreated and treated sweat, for product with fragrance B (3/5) followed by fragrance C (2/5).

In vivo self-assessment of deodorants:

We were particularly interested in A, B, C fragrances to correlate with electronic nose measurement.

According to notes and global assessment by volunteers, product B with better global note than A and C, presents a pleasant fragrance and a freshness evocation for 80% of volunteers. The intensity of fragrance was evaluated. The axe of improvement could be persistence of perfume in time.

This result is aligned with our observations with the electronic nose study where the B fragrance appears more efficient.

However, we noticed that the preferred formula was A, which reveals the importance of individual hedonic appreciation in such products including fragrance, despite the perceived efficacy.

Conclusion

With a step-by-step approach we developed a screening strategy to select components for an efficient anti humidity and anti-odor deodorant.

The classification of both absorption and desorption ability of several powders with a simple protocol allowed to make a first selection. The behavior of powders with humidity, can been observed at a microstructural level, thanks to real time monitoring ESEM for a better understanding and an appropriate choice.

The second step was to use a particular and still not very published electronic nose technology to compare fragrance efficacy in terms of odor covering. The development of the methodology was divided in 2 parts. Foremost, the study of sweat samples and their evolution, with the analysis of the olfactory profiles of sweat from several individuals. We clearly observed a variability between subjects, and a modification of the sweat signal in time, testifying of the presence of more volatile compounds, probably responsible for malodor. And Finally, we were then able to identify a way to appreciate fragrance proposals in terms of covering effect by their ability to transform the signal of odorant sweat.

The self-perception evaluation could give us confirmation of the fragrance selected in terms of global appreciation and warn us also to consider the panelist preference, which can differ from his efficiency evaluation.

Acknowledgments to

Romain Dubreuil, Etienne Bultel, Thierry Livache Aryballe Company,

Stéphane Desaint, Pierre Collin, Yves Rocher

Sabrina Ait-Said

Frédéric Nadaud – Université Technologie de Compiègne

Conflict of interest statement: NONE

References

- 1 Sato, K., & Sato, F. (1987). Sweat secretion by human axillary apocrine sweat gland in vitro. The American Physiological Society, R181-R187
- 2 M. Kanlayavattanakul, N. Lourith (2011). Body malodours and their topical treatment agents. International Journal of Cosmetic Science, 33, 298-311
- 3 D. Taylor, A.Daulby, S.Grimshaw, G. James, J. Mercer, S. Vaziri (2003). Characterization of the microflora of the human axilla. International Journal of Cosmetic Science, 25, 137-145